

Randomized Modulation of Power Converters via Markov Chains

Aleksandar M. Stanković, *Member, IEEE*, George C. Verghese, *Member, IEEE*, and David J. Perreault

Abstract—Randomized modulation of switching in power converters holds promise for reducing filtering requirements and reducing acoustic noise in motor drive applications. This paper is devoted to issues in analysis and synthesis of randomized modulation schemes based on finite Markov chains. The main advantage of this novel type of randomized modulation is the availability of an explicit control of time-domain performance, in addition to the possibility of shaping the power spectra of signals of interest. We focus on the power spectra of the switching functions that govern converter operation, and on the power spectra of certain associated waveforms. Numerical (Monte Carlo) and experimental verifications for our power spectral formulas are presented. We also formulate representative narrow- and wide-band synthesis problems in randomized modulation, and solve them numerically. Our results suggest that randomized modulation is very effective in satisfying narrow-band constraints, but has limited effectiveness in meeting wide-band signal power constraints.

Index Terms—Power electronics, Markov processes, switching circuits, modulation, spectral analysis, frequency-domain analysis, time domain analysis.

I. INTRODUCTION

SWITCHING power converters are designed to convert electrical power from one form to another at high efficiency. The high efficiency is obtained by using only switching devices, energy storage elements, and transformers (all of which are ideally lossless), and relying on appropriate modulation of the switches to convert the available ac or dc voltage/current waveforms of the power source into (approximately) the ac or dc waveforms required by the load. The switches are generally semiconductor devices: diodes, thyristors, bipolar junction transistors (operating at cutoff or saturation, not in their active region), MOSFET's, and so on. The engineering discipline devoted to this form of power conversion is called power electronics, see [11].

The conventional switching scheme for a switch in a power converter involves generating a (scaled version of a) switching function $q(t)$, which by definition has the value one when the switch is conducting, and the value zero otherwise. This is

Manuscript received March 15, 1995. Recommended by Associate Editor, J. Chiasson. The work of A. M. Stanković was supported by the National Science Foundation Grants ECS-9410354 and ECS-9502636, and by the ONR Grant 14-95-1-0723. Early work on this topic has been supported by the Digital Equipment Corp. and the MIT/Industry Power Electronics Collegium.

A. M. Stanković is with the Department of Electrical and Computer Engineering, Northeastern University, Boston, MA 02115 USA.

G. C. Verghese and D. J. Perreault are with the Laboratory for Electromagnetic and Electronic Systems, Massachusetts Institute of Technology, Cambridge, MA, 02139 USA.

Publisher Item Identifier S 1063-6536(97)00250-9.

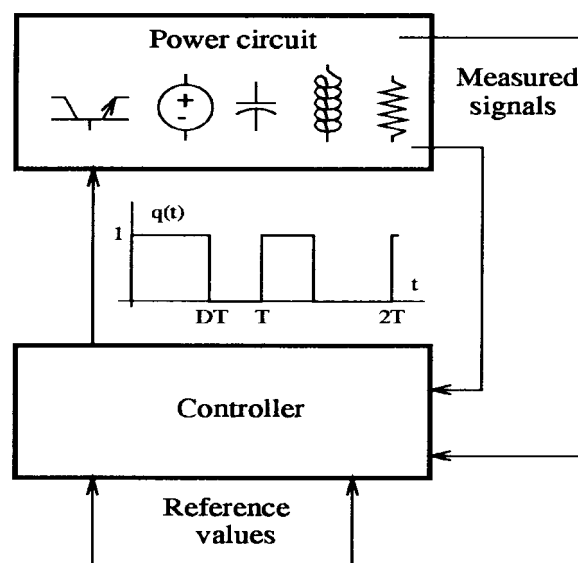


Fig. 1. Closed-loop control via modulation of the switching function.

schematically indicated in Fig. 1, which is drawn for the case of a converter in closed-loop operation.

In this scheme, the reference values fed to the controller reflect desired steady-state waveforms for the controlled voltages or currents. Any necessary feedback signals are combined with these reference values to determine $q(t)$. Since power converters generally operate in a periodic steady state, converter waveforms of interest are typically periodic functions of time in the steady state, as illustrated in Fig. 2. The average value, or *duty ratio* D , of $q(t)$ usually determines the nominal output of a dc/dc converter, while the fundamental component of $q(t)$ usually determines the output of a dc/ac converter; similar statements can be made for ac/dc and ac/ac converters.

Converter waveforms that are periodic have spectral components only at integer multiples of the fundamental frequency. The allowable harmonic content of some of these waveforms is often constrained; an example is the current in the interface to the electric utility, which ideally should have only the 60 Hz (or 50 Hz) fundamental component present. In this case, stringent filtering requirements may be imposed on the power converter. A significant part of a power converter's volume and weight can thus be due to an input or output filter. Similar requirements hold for acoustic noise control in motor applications. Harmonic components of the motor voltages and currents may excite mechanical resonances, leading to increased acoustic noise and to possible torque pulsations. Solutions to these problems include either a costly mechanical

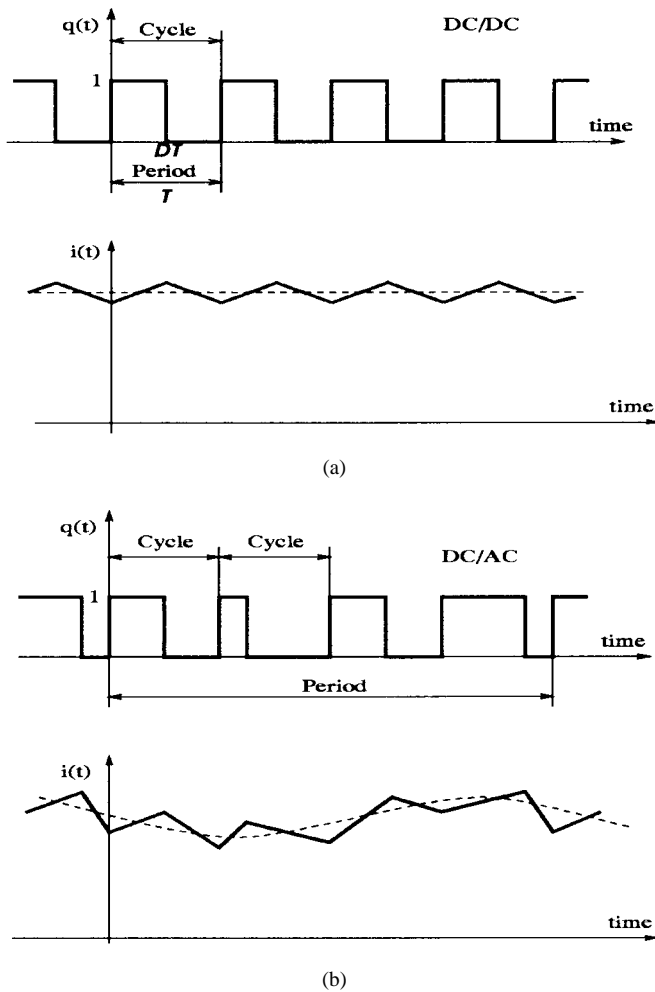


Fig. 2. Nominal switching function $q(t)$ and sample state variable $i(t)$ in two types of power converters: (a) dc/dc converter operating with duty ratio D ; (b) dc/ac converter.

redesign, or an increase in the switching frequency of the power converter supplying the motor, which in turn increases the switching power losses.

As the use of pulsewidth modulation (PWM) technology and microprocessors in power converters matured during the early 1980's, new methods became available to address the effects of acoustic noise in dc/ac converters supplying motors, and the effects of electromagnetic interference (EMI). While a substantial part of the engineering effort was directed toward the optimization of deterministic PWM waveforms ("programmed switching"), an alternative in the form of randomized modulation for dc/ac conversion was offered in [35]. The same idea has been pursued in a dc/dc setup in [32], and in numerous references afterwards, for example, [2]–[4], [7], [8], [13], [15]–[17], [25], [27], [31], [33], and [34]. The effect of the randomization is to attenuate the discrete spectrum, and introduce a continuous spectrum.

All prior results on randomized modulation in power electronics, with the exception of [28], are based on schemes in which successive randomizations of the switching pulse train (or of the periodic segments of this pulse train) are statistically independent and governed by invariant probabilistic rules. We denote such schemes as *stationary*. While

these implementations tend to be very successful in achieving certain kinds of spectral shaping in the frequency domain, they offer no guarantee or even description of the time-domain performance that accompanies the switching. This is objectionable in many cases, for example when accumulated deviations of the randomized switching waveform from the nominal (deterministic) waveform give rise to inadmissible variations in related currents and voltages. This problem, together with the lack of a widely known and accepted analysis framework for randomized switching waveforms, are among the main impediments to the wider use of randomized modulation.

In this paper we describe a generalization of the class of stationary randomized modulation schemes that enables explicit control of the time-domain performance of randomized switching, in addition to spectral shaping in the frequency domain. In this technique, the switching signal $q(t)$ comprises a concatenation of distinct waveform segments, chosen in sequence according to a Markovian model. In developing an analysis approach for this class of randomized signals, we present previous results from communication theory that are not well known outside that community, and develop some new results as well. We also pose and solve numerically certain synthesis problems that are formulated to assess the effectiveness of randomized modulation in achieving various performance specifications in the frequency domain.

To find a common ground for comparisons among different randomized modulation methods, we concentrate on the power spectrum of the switching function $q(t)$. The power spectra of variables related to $q(t)$ by linear time-invariant operations can easily be derived from the power spectrum of $q(t)$. Power spectra for waveforms that are not related to $q(t)$ by such operations take more effort to determine (some results are presented in [28]).

The basic *analysis* problem in randomized modulation is to relate the spectral characteristics of $q(t)$ and other associated waveforms in a converter to the probabilistic structure that governs the dithering of an underlying deterministic nominal switching pattern. The key *synthesis* problem in randomized modulation is to design a randomized switching procedure that minimizes given criteria for power spectra, while respecting various constraints, including those on time-domain behavior. Practically useful optimization procedures include the minimization of discrete spectral components (denoted as narrow-band optimization in [28]–[30]), and the minimization of signal power in a given frequency segment (denoted as wide-band optimization in [28]–[30]).

Section II describes a motivating example and introduces some notation. Section III recalls definitions of the autocorrelation and power spectrum for the class of signals of interest. Section IV discusses issues in numerical (Monte Carlo) verification of power spectral formulas. In Section V we describe and analyze randomized modulation based on Markov chains; details of derivations are in the Appendix. Section VI deals with synthesis problems in randomized modulation, and presents numerical results that suggest randomized modulation is well suited to meeting narrow-band constraints, but much less effective in satisfying wide-band constraints.

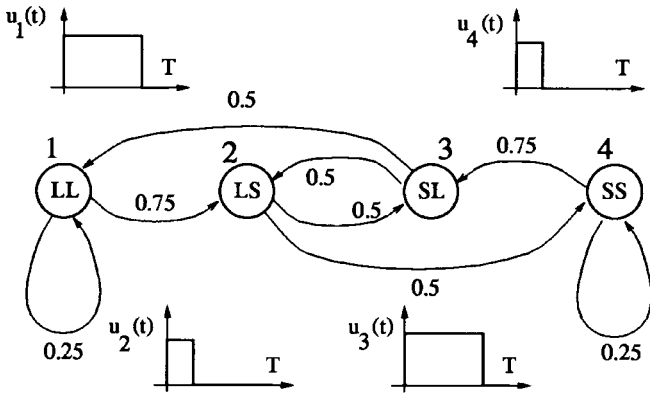


Fig. 3. An example of switching governed by an ergodic Markov chain.

II. AN EXAMPLE OF SWITCHING GOVERNED BY A MARKOV CHAIN

Consider the following switching scheme that could be used to randomize the operation of a dc/dc converter whose *average* duty ratio is required to be 0.5. Suppose we have two kinds of duty ratios D available: long, L, with $D = 0.75$; and short, S, with $D = 0.25$. The duty ratios have the desired average of 0.5, but we want to discourage long sequences of pulses of the same kind, thus preventing ripple buildup. We introduce a four-state Markov chain, corresponding to the following policy. The controller observes the two most recent switching cycles, and if they are SL or LS, then either of the pulses is fired with probability 0.5 for the next cycle. If the pair observed is LL, then an S pulse is applied with probability 0.75 (and an L pulse with probability 0.25). If the pair observed is SS, then an L pulse is applied with probability 0.75 (and an S pulse with probability 0.25). The chain is shown schematically in Fig. 3. The switching waveform $q(t)$ is generated by piecing together switching cycles ($u_k(t)$) corresponding to the states k successively visited by the chain, $k \in (1, \dots, 4)$. Note that this scheme offers additional flexibility when compared with switching based on statistically independent trials: we discourage runs of three pulses of the same kind, and can even completely prevent such runs (by setting the appropriate probabilities to 0).

For the four-state Markov chain in Fig. 3, we define P as the 4×4 state-transition matrix, and its (k, l) th entry is the probability that at the next transition the chain goes to state l , given that it is currently in state k

$$P = \begin{bmatrix} 1/4 & 3/4 & 0 & 0 \\ 0 & 0 & 1/2 & 1/2 \\ 1/2 & 1/2 & 0 & 0 \\ 0 & 0 & 3/4 & 1/4 \end{bmatrix}. \quad (1)$$

Note that each row of P sums to 1; P is thus a stochastic matrix, and therefore has a nonrepeated eigenvalue $\lambda_1 = 1$ (with corresponding right eigenvector $\mathbf{1}_4 = [1 \ 1 \ 1 \ 1]^T$) and all other eigenvalues with moduli strictly less than one. The steady-state probabilities corresponding to P , which can be interpreted as the fraction of a (large) total number of state

transitions that the chain spends in state k , are solutions to

$$\Pi P = \Pi, \quad \sum_{k=1}^4 \Pi_k = 1 \quad (2)$$

and equal $\Pi = [0.2 \ 0.3 \ 0.3 \ 0.2]$. Thus Π is the left eigenvector of P corresponding to eigenvalue $\lambda_1 = 1$. For later use we define the vector of switching cycles

$$\mathbf{u}(\tau_1) = \begin{bmatrix} u_1(\tau_1) \\ u_2(\tau_1) \\ u_3(\tau_1) \\ u_4(\tau_1) \end{bmatrix}, \quad 0 \leq \tau_1 \leq T \quad (3)$$

where in the example $u_1(\tau_1) = 1$ for $0 \leq \tau_1 \leq (3/4)T$ and $u_1(\tau_1) = 0$ for $(3/4)T \leq \tau_1 \leq T$, etc. Our goal is to characterize the switching waveform $q(t)$ in the frequency domain.

III. AUTOCORRELATION AND POWER SPECTRUM

A. Basic Definitions

A *random signal* may be thought of as a signal selected from an ensemble (family) of possible signals by a random experiment governed by some specification of probabilistic structure. The ensemble of signals and the specification of probabilities together comprise the *random process* (or stochastic process) generating the random signal.

The *time-average autocorrelation* [20], [24], [36] of a random process $q(t)$ is defined as

$$R_q(\tau) = \lim_{W \rightarrow \infty} \frac{1}{2W} \int_{-W}^W E[q(t)q(\tau+t)] dt \quad (4)$$

where the expectation $E[\cdot]$ is taken over the whole ensemble, $[\cdot]$. The process is termed quasi stationary [20] (or asymptotically mean stationary, [19]) if this limit and a similar one for $E[q(t)]$ exist; we shall assume throughout that $q(t)$ is quasi-stationary. (Such processes are more general than wide-sense stationary processes, where the time averaging is not needed to get a result independent of t .) This definition is applicable to deterministic signals as well, since for deterministic signals the ensemble consists of a single member. The (mean or average) *power density spectrum* $S_q(f)$ is then defined as the Fourier transform of $R_q(\tau)$

$$S_q(f) = \int_{-\infty}^{\infty} e^{-j2\pi f\tau} R_q(\tau) d\tau. \quad (5)$$

From this definition $S_q(-f) = S_q(f)^*$ since $R_q(\tau)$ is real, so we will only consider $f \geq 0$ in the sequel. In cases of practical interest, $S_q(f)$ can have a continuous and an impulsive part [5]. The impulsive part of $S_q(f)$ is referred to as the *discrete* spectrum, and is characterized entirely by the locations f_1, f_2, \dots of the impulses (“line frequencies” and “harmonic frequencies”) and by positive numbers p_1, p_2, \dots representing the strengths of the impulses (i.e., the signal power at the harmonic frequencies). Integrating $S_q(f)$ over a frequency range yields the signal power in that frequency range.

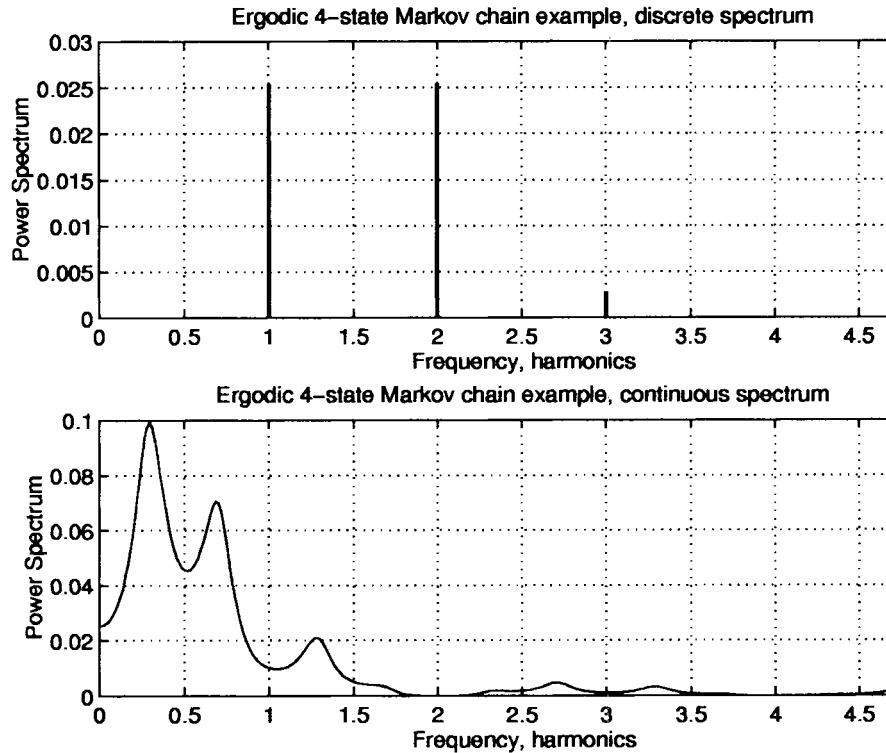


Fig. 4. Calculated power spectrum of $q(t)$ for the Markov chain example of Section II.

B. Power Spectra and Linear Systems

An important result for applications is the transformation of the autocorrelation when a process $x(t)$ with autocorrelation $R_x(\tau)$ passes through a linear, time invariant filter. The filter is characterized by its impulse response $h(t)$ and corresponding frequency response $H(f)$, which is the Fourier transform of $h(t)$. The output $y(t)$ of the system is given by convolution

$$y(t) = \int_{-\infty}^{\infty} x(t)h(t-u) du. \quad (6)$$

Using this relation it can be shown [36] that the process $y(t)$ has a well defined autocorrelation, given by (4), and that its power spectrum is

$$S_y(f) = |H(f)|^2 S_x(f). \quad (7)$$

This relation can be used in our setting to evaluate the power spectrum of any waveform related to the switching waveform $q(t) = x(t)$ through a convolution, once the power spectrum of $q(t)$ is known. The relation (7) holds whenever the integral of the right-hand side over all frequencies is finite; although bounded-input bounded-output (BIBO) stability of the filter suffices for this, BIBO stability is not necessary [36, pp. 487–490].

Let $X_{2W}(f)$ denote the Fourier transform of the symmetrically truncated version of $x(t)$, extending from $-W$ to $+W$ in time. An important result of the Fourier theory [5], [18] due to the Einstein–Wiener–Khinchine theorem, shows that

$$S_x(f) = \lim_{W \rightarrow \infty} E \left(\frac{1}{2W} |X_{2W}(f)|^2 \right). \quad (8)$$

The quantity $(1/2W)|X_{2W}(f)|^2$ is called the *periodogram* of $x(t)$. For nonstationary processes that have a well-defined autocorrelation via (4) the equality in (8) is in the sense of distributions [5], [20], [36].

IV. VERIFICATION ISSUES

The formulas that will be developed shortly for power spectra of different randomized modulation schemes are rather involved, and a need arises to verify and explore them through simulation. (We also provide experimental verification in some cases.) The power spectrum of a (Monte Carlo) simulation of a randomized switching waveform $q(t)$ is obtained through an estimation procedure. Power spectrum estimation is one of the most important problems in signal processing and has a very rich history [20], [21], [24], [26], [33].

The discussion in this section deals primarily with direct estimation methods that yield the power spectrum $S_q(f)$ without estimating the autocorrelation. We concentrate on nonparametric, classical estimation methods, which are well understood and for which software is readily available [26].

Classical direct estimation methods may be thought of as approximate implementations of the operations specified in the Einstein–Wiener–Khinchine theorem (8). Typically, a single realization of the process of length $2KW$ is divided into K sections, and the (discrete-time) periodogram is computed for each section (from closely spaced time samples of the signal). The availability of the fast Fourier transform (FFT) to calculate the Fourier transforms involved is a major advantage. The expectation operation in (8) is then approximated by averaging the K individual periodograms. This approach is referred to as Bartlett's method. Under appropriate conditions

(related to ergodicity of the stochastic process, which permits time averages to be substituted for ensemble averages) this computation produces a consistent, asymptotically unbiased estimate of the power spectrum [10], [26], so the estimate converges to the true spectrum as $K \rightarrow \infty, W \rightarrow \infty$. We shall assume that the switching functions $q(t)$ of interest to us satisfy the conditions required for validity of such an estimation procedure. The close match that will be demonstrated between our analytical formulas and the Monte Carlo verifications suggest that this is indeed a good assumption.

Although the above estimation procedure is asymptotically unbiased, in practice K and W are finite, so there is inevitable bias. The use of appropriate windows in the time domain contributes to bias reduction. An unpleasant effect of windowing is known as leakage and has its source in the side-lobes (in the frequency domain) of the windows used. Leakage results in loss of resolution in the estimates. Welch's modification of Bartlett's method, [26], allows data segments to overlap in addition to windowing data in the time domain. This method is widely used and is available in the Matlab software package. A more detailed discussion of verification problems is presented in [28].

V. MODULATION BASED ON MARKOV CHAINS

A. Switching Governed by Markov Chains

In this section we consider the class of randomized modulation schemes introduced via the example in Section II. A switching waveform segment of length T_k is associated with the Markov chain being in the k th state, $k \in 1, \dots, n$. Concatenation of these segments yields a continuous-time switching (0–1) waveform $q(t)$ that is associated with the evolution of the chain. The first task is to establish relations linking the discrete-time Markov chain with the continuous-time switching function $q(t)$. This connection is complicated by the fact that the durations T_k of switching cycles corresponding to individual states of the chain could be different. If the lengths of the cycles are equal for all states, (i.e., $T_k = T$ for all k), the chain is called *synchronous* (i.e., $T_k = T$ for all k); otherwise, the chain is denoted as *asynchronous*.

We briefly review some definitions and results from the field of Markov chain analysis. For a complete review, see, for example, [9], [14], and [18]. A slightly different nomenclature is used in [12]. A Markov chain is *irreducible* if every state can be reached from every other state. The state k is *recurrent* (or *essential*) if the chain can eventually return to k from every state that may be reached from k ; every state in an irreducible chain is therefore recurrent. A recurrent state to which the chain can return only after an integer multiple of d transitions ($d \geq 2$) is called a *periodic state*, with period d . The property of irreducibility, which is assumed in this paper, implies that all periodic states have the same period.

A Markov chain with finitely many states is classified as *ergodic* if it is irreducible and aperiodic (i.e., has no periodic states) [14]. In this case limiting state probabilities exist, the limiting state probability Π_k of the state k being the probability that the chain is in state k after a great many state transitions.

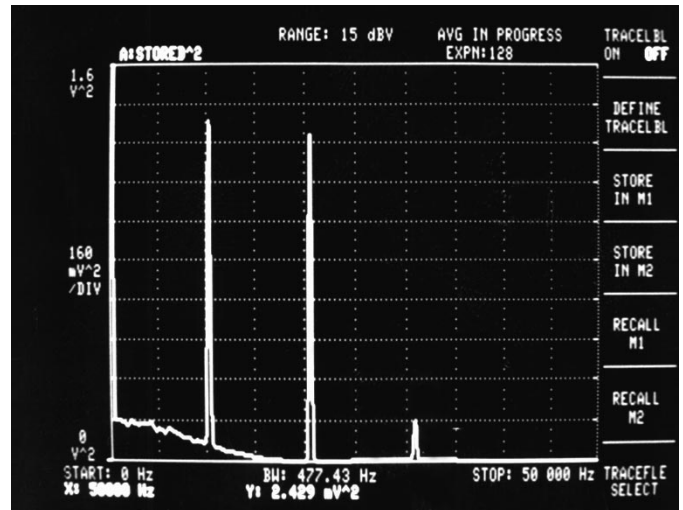


Fig. 5. Measured power spectrum of $q(t)$ for the Markov chain example.

This quantity is independent of the initial state under ergodicity assumptions.

Some analysis results for waveforms generated in the fashion described here have been provided by communication theorists [6], [37], but applications in power electronics have not been suggested before. The case of inverter (dc/ac) modulation based on Markov chains requires results that do not seem to be in the communication theory literature either; our results for this case were derived in [28], and are presented later in this paper. A development relevant for dc/ac converters is the study of a particular category of periodic (but possibly asynchronous) Markov chains. The n states are divided into N classes, and state transitions of the underlying discrete-time Markov chain are constrained to occur from one class to the next ($k \rightarrow k+1, 1 \leq k < N$, and from the N th class to the first). In this case, limiting state probabilities as defined earlier do not exist (they do exist, however, conditioned on knowledge the class in which the chain is located). This setup represents a generalization of the block-stationary independent randomized modulation analyzed in [28]–[30]. One can think of each class having approximately the local average needed in a part of the the ac waveform (e.g., pulsewidth modulated approximation of a sinusoid), while the switching cycles within a class differ in other features (e.g., pulse position).

B. Power Spectra Generated by Ergodic Markov Chains

Ergodic Markov chains (i.e., irreducible and aperiodic chains) are considered in this section. Our goal is to analyze the continuous-time switching waveforms associated with an n -state discrete-time Markov chain. As in the example in Section II, the chain is characterized by the $n \times n$ state transition matrix P and by the corresponding steady-state probabilities Π . We allow switching cycles generated in different states to have different lengths T_k , but require that these be integer multiples of a greatest common divisor \hat{T} (i.e., $T_k = \ell_k \hat{T}, \ell \in \mathbb{N}$). We also define $T_M = \max(T_k), T_m = \min(T_k)$ and $\tilde{T} = \sum_{k=1}^n \Pi_k T_k$. Note that \tilde{T} is the expected time between transitions. Let the 0–1 waveform in the

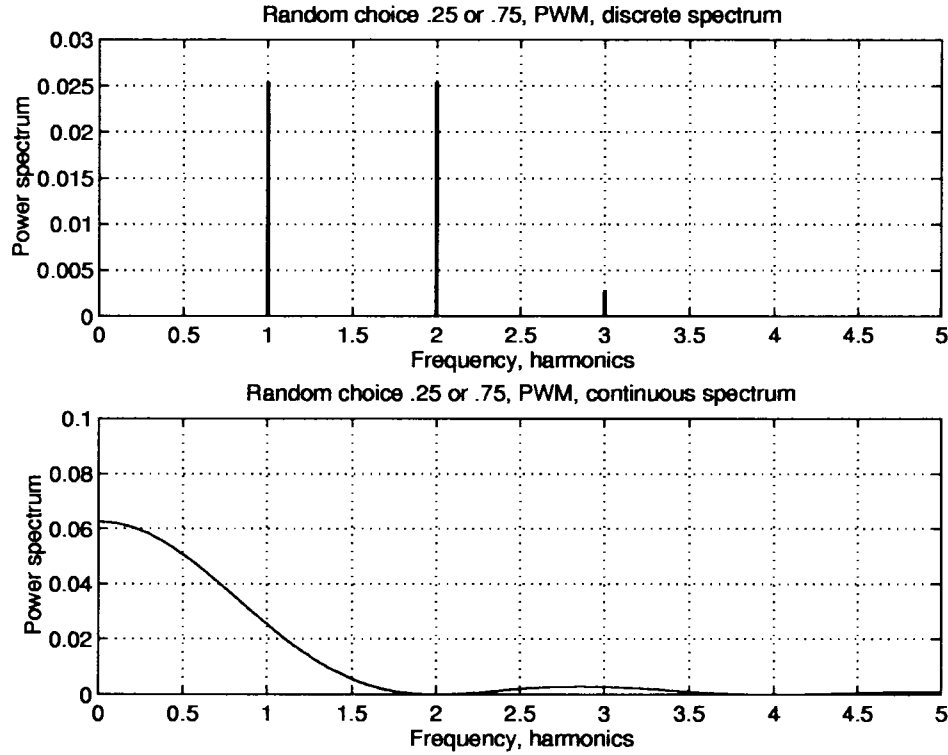


Fig. 6. Calculated power spectrum of $q(t)$ for the randomized PWM example.

switching cycle of duration T_k associated with the state k be $u_k(\cdot)$, and let $u(\cdot)$ be an n -vector with entries $u_k(\cdot)$.

The main task is to find the autocorrelation of the continuous-time waveform generated by the Markov chain, using the formula (4). We shall assume (without loss of generality) that a particular realization of $q(t)$ contains $2N$ whole pulses in a window of duration $2W$. The contribution of the fractional pieces within $2W$ to $R_q(\tau)$ will tend to zero as $N \rightarrow \infty$, so (4) becomes

$$R_q(\tau) = \lim_{N \rightarrow \infty} \frac{1}{2NT} \int_{2NT}^{2NT+2T} E[q(t)q(\tau+t)] dt \quad (9)$$

where the average pulse length is \tilde{T} [22].

Due to its technical nature, the detailed derivation of our spectral formulas is given in the Appendix. To present the results here, let us introduce the following notation: $U(f)$ is the Fourier transform of the n -vector $u(\cdot)$ of waveforms $u_k(\cdot)$ associated with various states; $\Theta = \text{diag}(\Pi)$; $\hat{Q}(f) = \text{diag}(e^{-j2\pi f T_k})P$; $G(f) = (I - \hat{Q}(f))^{-1}$ (where defined). The end result for the continuous power spectrum is

$$S_{cq}(f) = U(f)^H [\Theta G(f) + (\Theta G(f))^H - \Theta] U(f) \quad (10)$$

while the final result for the intensities of the impulses ("lines" in the discrete spectrum) is

$$S_{dq}\left(\frac{k}{\tilde{T}}\right) = \frac{1}{\tilde{T}^2} \left| \Pi U\left(\frac{k}{\tilde{T}}\right) \right|^2 \quad k \in \mathbb{N}. \quad (11)$$

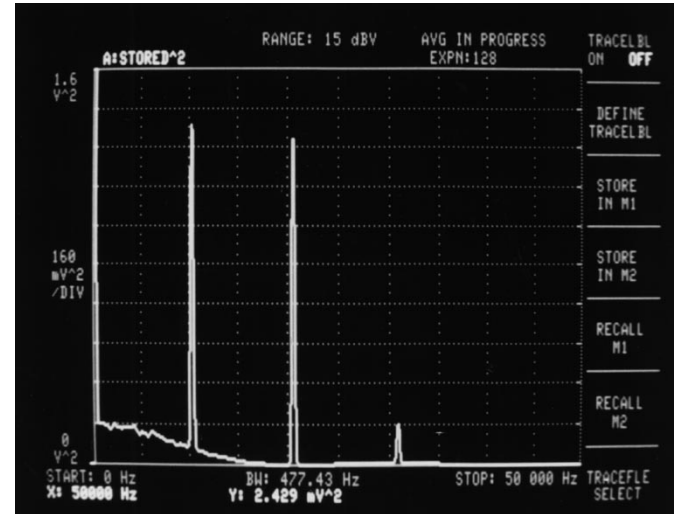


Fig. 7. Measured power spectrum of $q(t)$ for the randomized PWM example.

1) *Example of Switching Governed by Ergodic Markov Chain:* Next we evaluate the preceding expressions for power spectra on the four-state example introduced in Section II. The theoretical discrete and continuous spectra corresponding to our example are shown in Fig. 4, where unit frequency corresponds to the switching frequency. The measured power spectrum in the same case is shown in Fig. 5. The circuit used for experimental verification was a modified buck converter (without the output capacitor), and the nominal switching frequency was 10 kHz. We focus on the switching function, and it is not influenced by details of the circuit topology

(related waveforms such as input and output voltages and currents do depend, however, on the circuit topology). Our experiments suggest that randomized modulation schemes based on Markov chains are not more difficult to implement than the schemes reported in the literature for stationary randomized modulation. For example, one only needs a two-bit random number generator and a state counter to implement the Markov chain of this example.

The results can be compared with deterministic switching at a constant duty ratio of 0.5, in which case only the discrete spectrum exists, with a first harmonic of $1/\pi^2 = 0.1013$, (and subsequent odd harmonics reduced by $1/n^2$). Another meaningful comparison is with a randomized PWM scheme in which a random choice is made at each trial between duty ratios of 0.25 and 0.75, independently of previous outcomes. Results for randomized PWM can be found in [22], [28]. Formulas (10) and (11) can also be applied to the corresponding two-state Markov chain in which all transition probabilities are equal to 0.5. Calculated and measured spectra in this case are shown in Figs. 6 and 7. The experimental setup was the same as in the case of randomized switching governed by a Markov chain.

While the two schemes are quite similar in terms of their power spectra, their time-domain performance is very different. As an example, let us consider the event “five successive long (L) pulses” in both schemes. This event could be of interest, since it is associated with a fairly large net buildup of the local duty-ratio. In the case of independent randomized PWM, the probability of “five L in a row” is $(1/2)^5 = 0.03125$. In the case of modulation based on the Markov chain from the example, the probability of the same event equals $0.2 \times (1/4)^3 = 0.003125$ [28], i.e., it is reduced ten times. These results have been verified both in simulations and in an actual circuit implementation. This example illustrates the power of Markov chain modulation, which achieves the shaping of the power spectrum, while enabling control of the time-domain waveforms. Other variations are possible. For example, an S pulse could be *required* after an LL pair has been observed in the last two pulses (and symmetrically for an SS pair), thus altogether preventing the occurrence of more than two pulses of the same sort.

C. Periodic Markov Chains

The case of pulse trains specified by a class of *periodic* Markov chains is considered in this section. This class is denoted as *ergodic cyclic* in some places [12]. A related result for the special case of synchronous Markov chains is given in [6]. We assume that the state of the chain goes through a sequence of \hat{N} classes of states C_l , occupying a state in each class for an average time $\tilde{T}_l, l = 1, \dots, \hat{N}$. In the power electronic setup, periodic Markov chains are of interest in randomized modulation for dc/ac applications, where the basic (reference) single-cycle on-off pattern changes from one cycle to the next in a deterministic fashion. This pattern is further dithered in each cycle using a set of dependent (Markovian) trials in order to satisfy time-domain constraints (for example to control the “ripple” of waveforms of interest).

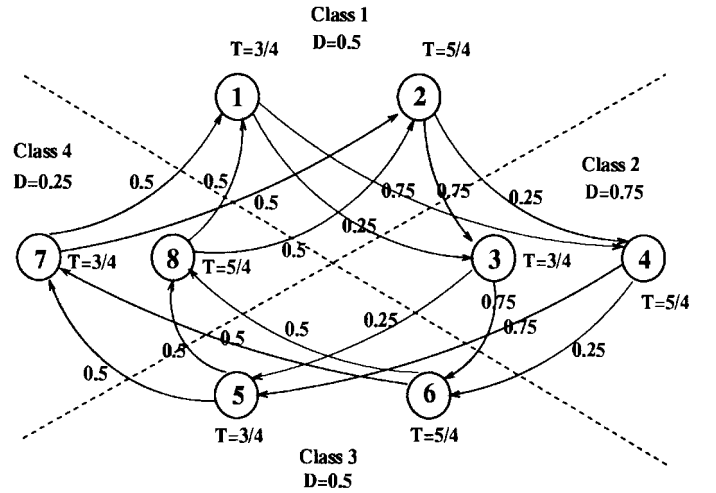


Fig. 8. Periodic Markov chain with eight states and four classes.

The conditioning used in the derivation of the power spectrum formula in the previous subsection (and detailed in the Appendix) has to be adjusted in the following way. The contribution that states of the Markov chain belonging to the class C_k make to the time-averaged autocorrelation (4) is scaled by $\tilde{T}_k / \sum_{l=1}^{\hat{N}} \tilde{T}_l$, where \tilde{T}_l is the expected time spent in the class C_l before a transition into the class C_{l+1} (we evaluate these quantities later).

It can be shown (e.g., in [1]) that after a possible renumbering of the states, the matrix P (and Q , see the appendix) for a periodic Markov chain can be written in a block-cyclic form

$$P = \begin{bmatrix} 0 & P_{12} & 0 & \cdot & 0 \\ 0 & 0 & P_{23} & \cdot & 0 \\ \cdot & \cdot & \cdot & \cdot & \cdot \\ 0 & 0 & 0 & \cdot & P_{\hat{N}-1, \hat{N}} \\ P_{\hat{N}, 1} & 0 & 0 & \cdot & 0 \end{bmatrix}.$$

Let P_1 denote the product of submatrices of P in the following order: $P_1 = P_{\hat{N}, 1} \dots P_{23} P_{12}$, and let Π^1 denote the vector of the steady-state probabilities, conditional on the system being in class C_1 . Then

$$\Pi^1 = \Pi^1 P_1 \quad (12)$$

and the average time spent in class C_1 is $\tilde{T}_1 = \sum_k \Pi_k^1 T_k$, where the summation is taken over all states in class C_1 .

Let $\tilde{T} = \sum_{l=1}^{\hat{N}} \tilde{T}_l$, and let $\Theta_k = \text{diag}(\Pi^k)$. The conditioning procedure used in the Appendix, based on the number of transitions \hat{m} between τ_1 and $\tau_1 + \tau$, will be used again, with the following modification. If the first pulse belongs to the class k , then the pulse straddling $\tau_1 + \tau$ belongs to the class $(k + \hat{m}) \bmod \hat{N}$. When we add the contributions of all classes to the average power spectrum (scaled by the relative average duration of each class, as illustrated in the Appendix), the result can be written in the following compact form:

$$S_q(f) = \frac{1}{\tilde{T}} \left[\sum_{k=1}^{\hat{N}} \frac{\tilde{T}_k}{\tilde{T}} U_k^H(f) \Theta_k U_k(f) + 2 \text{Re}(\mathbf{1}_{\hat{N}}^T S_c \mathbf{1}_{\hat{N}}) \right] + \frac{1}{\tilde{T}^2} \text{Re}(\mathbf{1}_{\hat{N}}^T S_d \mathbf{1}_{\hat{N}}) \sum_{l=-\infty}^{\infty} \delta\left(f - \frac{l}{\tilde{T}}\right) \quad (13)$$

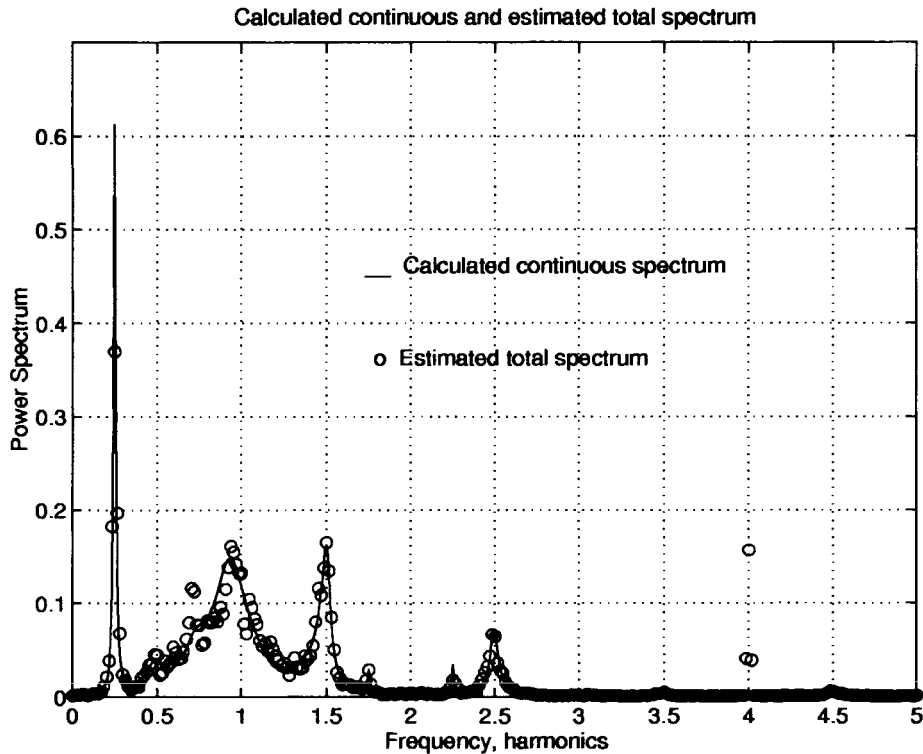


Fig. 9. Estimated and calculated spectrum for the periodic Markov chain in Fig. 8 with eight states and four classes.

where \hat{T} is the greatest common divisor of all waveform durations, $\mathbf{1}_{\hat{N}}$ is an $\hat{N} \times 1$ vector of ones and U_k is the vector of Fourier transforms of waveforms assigned to states in class C_k . A circular indexing scheme (i.e., modulo \hat{N}) is used in this subsection.

The matrix S_c has a Toeplitz structure, with (k, l) th entry

$$S_{ck,l}(f) = \frac{\hat{T}_k}{\hat{T}} U_k^H(f) (I - \Lambda_k(f))^{-1} \Lambda_{k,l}(f) U_l(f) \quad (14)$$

where Λ_k is a product of \hat{N} matrices

$$\Lambda_k = Q_{k-1,k}, \dots, Q_{k,k+1}$$

and

$$\Lambda_{k,l} = Q_{l-1,l}, \dots, Q_{k,k+1}$$

with no repetitions allowed in $\Lambda_{k,l}$, so that the number of matrices forming $\Lambda_{k,l}$ is $\hat{N} - |k - l|$. Also, the (k, l) th entry of S_d

$$S_{dk,l}\left(f = \frac{l}{\hat{T}}\right) = \frac{\hat{T}_k}{\hat{T}} U_k^H\left(f = \frac{l}{\hat{T}}\right) \Pi^k (\Pi^l)^T U_l\left(f = \frac{l}{\hat{T}}\right). \quad (15)$$

The result (13) appears to be novel [28], and it will be now verified via an example.

1) *Example of Switching Governed by a Periodic Markov Chain:* In this example we consider a simplification of a switching scheme applicable to dc/ac converters. The goal is to generate a switching function in which blocks of pulses have nominal (deterministic) duty ratios

$$[0.5, 0.75, 0.5, 0.25],$$

This may correspond to a (very crude) approximation of a sinusoid. When randomizing this pattern, it is desirable to prevent large deviations from the values in the corresponding deterministic pulse train (i.e., the one with the above duty ratios and all blocks of the fixed shape). The periodic Markov chain shown in Fig. 8, with eight states divided into four classes, is an example of a solution to such a design problem. In this case a short (duration 3/4) and a long (duration 5/4) cycle is available in each of the four classes; in classes 1 and 2 the transition pattern favors patterns in which the two types alternate. We analyze this chain using (13), and in Fig. 9 we compare the theoretical predictions for the continuous spectrum (solid line) with estimates of the total spectrum obtained via Monte Carlo simulations (circles). The agreement between the two is quite satisfactory; the theoretical prediction for the impulse strength at $f = 4$ is 0.0036, which agrees well with the estimated value of 0.0037. In Fig. 10 we show the experimentally observed power spectrum for the same periodic Markov chain. An application of (13) for Markov chains with many more classes of states could become computationally intensive. This is not a major drawback, however, due to the off-line character of the calculation. Our experience suggests that a real-time implementation of switching based on a Markov chain is not necessarily more complicated than conventional "programmed" switching, especially if the transition probabilities are of the form $(1/2)^b$, where b is the number of (random) bits needed for the Markov chain implementation.

VI. SYNTHESIS PROBLEMS

In this section the goal is to explore how effective randomized modulation is in achieving various performance specifica-

TABLE I
NARROW-BAND OPTIMIZATION, CRITERION VALUES ($\times 10^{-4}$)

Modulation	Probabilities	J_1^{NB}	$J_{1,41}^{NB}$
Randomized PWM	Independent, $D_1 = 0.25, D_2 = 0.75$	253	613
Standard Markov Chain	$p_{1,2} = .75, p_{2,3} = .5, D_1 = 0.25, D_2 = 0.75$	253	613
Optimal Markov Chain	$p_{1,2} = .75, p_{2,3} = .5, D_1 = 0.05, D_2 = 0.95$	0	11.5

TABLE II
WIDE-BAND OPTIMIZATION, CRITERION VALUES ($\times 10^{-4}$)

Modulation	Probabilities	J_1^{WB}
Randomized PWM	Independent, $D_1 = 0.25, D_2 = 0.75$	800
Standard Markov Chain	$p_{1,2} = .75, p_{2,3} = .50, D_1 = 0.25, D_2 = 0.75$	806
Optimal Markov Chain	$p_{1,2} = .05, p_{2,3} = .95, D_1 = 0.22, D_2 = 0.77$	786

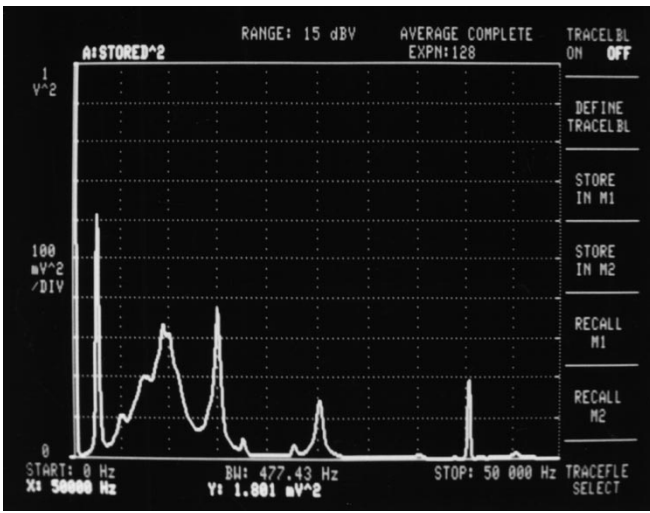


Fig. 10. Measured power spectrum for the periodic Markov chain of Fig. 8.

tions in the frequency domain. Desirable properties of power spectra are dependent on the particular application. Requirements of particular interest in practice are the following.

- Minimization of one or multiple, possibly weighted, discrete harmonics. This criterion corresponds to cases where the narrow-band characteristics corresponding to discrete harmonics are particularly harmful, as for example in acoustic noise, or in narrow-band interference in communication systems.
- Minimization of signal power (integral of the power spectrum) in a frequency segment that is of the order of an integral multiple of the switching frequency. This criterion corresponds to wide-band constraints in military specifications, and it could be of interest for EMI problems.

A typical narrow-band optimization criterion is a weighted sum of discrete harmonic intensities between the l th and L th harmonics, and is denoted as $J_{l,L}^{NB}$. A reasonable wide-band optimization criterion, used for illustration in this section, corresponds to the minimization of the signal power in the frequency segment $[0, 1.5]$, where the average switching frequency is one.

The optimization process has to address two related issues:

- 1) Design of an n -state Markov chain (possibly periodic), which reduces to the specification of a stochastic matrix P ;
- 2) Choice of n 0–1 functions, each supported on $[0, T_k]$, that correspond to distinct cycles of the switching function.

While the criterion functions are defined in the frequency domain, the design is performed in the time-domain. This makes the optimization problem difficult, and we present and comment on numerical results. A complete parameterization in the frequency domain of all candidate functions is not known, even for the much simpler case of stationary random modulation [28]–[30].

Synthesis problems for randomized modulation governed by Markov chains will be illustrated on the example from Section IV-B1. The transition probabilities $p_{1,2}$ from state 1 to state 2, and $p_{2,3}$ from state 2 to state 3 will be optimized, while the symmetry of the chain is preserved. Thus the transition matrix is

$$P = \begin{bmatrix} p_{1,2} & 1 - p_{1,2} & 0 & 0 \\ 0 & 0 & p_{2,3} & 1 - p_{2,3} \\ 1 - p_{2,3} & p_{2,3} & 0 & 0 \\ 0 & 0 & 1 - p_{1,2} & p_{1,2} \end{bmatrix}. \quad (16)$$

The duty ratios of the short and long pulses are also made variable, with the same average value $D = 0.5$ as in the original example. The optimized narrow-band criteria are shown in Table I. Thus a considerable improvement in criterion value is attained as a consequence of optimization.

It is evident from Table II that switching based on a Markov chain is not particularly effective in reducing wide-band signal power. The purpose of our optimization procedures is to point out salient capabilities of randomized modulation governed by Markov chains, and consequently our searches were performed over granular grids. In the numerical experiments reported here, as well as in examples with average duty ratios different from 0.5, the duty ratio variations seem to be most effective in dealing with narrow-band constraints. This fact is expected from the performance analysis of stationary schemes [28]. Also, transition matrix variations have effects mostly on wide-band criteria, but their overall effectiveness is limited. The true

importance of the transition matrix optimization is in the time domain, where it influences the ripple.

These results suggest a decomposition of the Markov chain optimization problem into two subproblems. The first subproblem is the transition matrix optimization, and it is concerned mostly with time domain requirements (ripple control), and to a certain extent with the wide-band constraints in the frequency domain. The second subproblem is the optimization of the waveforms at each state, and its primary effects are in satisfying the narrow-band requirements. The proposed decomposition could significantly improve the tractability of the optimization of Markov chains with many states.

VII. CONCLUSIONS

In this paper we have presented analysis and synthesis results for randomized modulation strategies governed by Markov chains, suitable for different classes of power converters. Randomized modulation switching schemes governed by Markov chains that are applicable to dc/dc and dc/ac converters have been described and analyzed. Our spectral formulas for periodic Markov chains are believed to be novel. Synthesis problems in randomized modulation have also been considered, where both optimization criteria and numerical results are described. It is shown that randomized pulse modulation can be very efficient in reducing the size of discrete harmonics and in satisfying narrow-band constraints, but is much less effective in dealing with wide-band requirements.

APPENDIX

In this section we provide a derivation of spectral formulas for ergodic Markov chains. A synopsis is as follows: after introducing some notation, the proof outline contains five main steps: in the first we derive an expression for the autocorrelation conditioned on the number of state transitions of the governing Markov chain; in the second step we obtain a formula for the part of the power spectrum corresponding to positive delay τ in the autocorrelation. At this point we arrive at an expression involving an infinite matrix sum, and we present relevant eigenvalue considerations in the third step. In the fourth step we derive an expression for the continuous part of the power spectrum, and in the fifth step we obtain a formula for the discrete part.

Let M denote the number of state transitions in our $2N\tilde{T}$ -truncated realization (as noted before, $M \leq 2N\tilde{T}/T_m + 1$). Note that due to the ergodicity of the Markov chain the asymptotic behavior of M is $M\tilde{T}/2W \rightarrow 1$, as $W \rightarrow \infty$. A typical waveform is shown in Fig. 11.

Step 1: For the integral in (9), t ranges over cycles of each of the n types. We first separate this integral to display the contribution due to t lying in cycles of type k for each $k \in [1, n]$. Next, we use the law of large numbers for irreducible Markov chains [12, Th. 4.2.1, pp. 73–74] to obtain

$$R_q(\tau) = \frac{1}{\tilde{T}} \sum_{k=1}^n \Pi_k A_q^k(\tau) \quad (17)$$

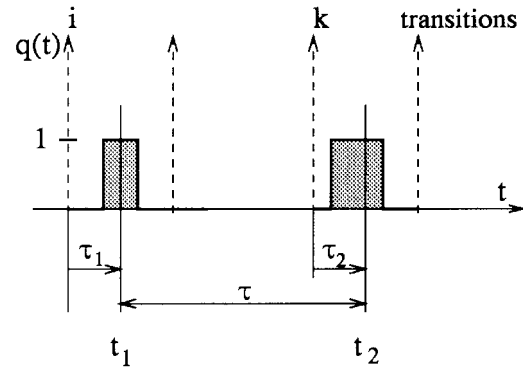


Fig. 11. Notation for the switching waveform generated by a Markov chain.

where

$$A_q^k(\tau) = \int_0^{T_k} E[q(\tau_1)q(\tau + \tau_1)|k] d\tau_1. \quad (18)$$

We have used the symbol $E[\cdot|k]$ to denote the expectation conditioned on the *first* pulse being of type k , and we use the symbol τ_1 to denote the epoch (point in time) relative to the beginning of the first pulse (see Fig. 11—we assume in this derivation that both pulses in Fig. 11 are within the window of length $2N\tilde{T}$, which yields correct results in the limit). We shall use τ_2 to denote the epoch relative to the start of the cycle straddling the instant $\tau_1 + \tau$. Then $E[q(\tau_1)q(\tau + \tau_1)|k] = u_k(\tau_1)E[q(\tau + \tau_1)|k]$. Given that $u_k(\tau_1) = 0$ for $\tau_1 > T_k$, the value of $A_q^k(\tau)$ will not change if the integration is performed from zero to T_M , (recall that $T_M = \max(T_k)$). This property holds for all integrals involving integrands that are products of $u_k(\cdot)$ with other functions.

Let us consider an experiment in which we fix τ_1 and τ we observe the number \hat{m} of state transitions between τ_1 and $\tau_1 + \tau$. It is finite for any finite τ (since all T_k are finite), and moreover it forms an event space, as different \hat{m} are mutually exclusive and collectively exhaustive events. We will be using this result to evaluate $A_q^k(\tau)$ by using additivity of probabilities of events conditioned on \hat{m} . If $\tau > 0$

$$A_q^k(\tau) = A_q^k(\tau|\hat{m} = 0) + \sum_{m=1}^M A_q^k(\tau|\hat{m} = m) \quad (19)$$

where $A_q^k(\tau|\hat{m} = m)$ denotes the contribution to the expectation in the case when $\hat{m} = m$, and M can be chosen as $M = \tau/T_m + 1$ (recall that $T_m = \min(T_k)$). We shall consider the first term, with $\hat{m} = 0$, later.

Observe that the main difficulty in our calculation of $A_q^k(\tau)$ is the calculation of the ensemble average $u_k(\tau_1)E[q(\tau + \tau_1)|k]$, due to the Markovian dependence of successive pulses. Referring to Fig. 11, given τ and the number of state transitions \hat{m} during τ , only certain epochs τ_2 are possible for the pulse that straddles the instant $\tau_1 + \tau$. Note that τ_2 is a discrete random variable that satisfies $\tau_2 \in [0, T_M]$, and whose probability mass function depends on the trajectory of the chain. To keep track of both the possible range of τ_2 and of the associated probabilities of the pulse that straddles $\tau_1 + \tau$ being of type l , we will introduce an $n \times n$ matrix $Q(\sigma)$ whose

(k, l) th entry is $Q_{k,l}(\sigma) = P_{k,l}\delta(\sigma - T_k)$. We can thus write

$$Q(\sigma) = \text{diag}(\delta(\sigma - T_k))P = \Delta(\sigma) \cdot P.$$

In the example from Section II, $Q(\sigma) = \text{diag}(\delta(\sigma - T))P$. The expectation $E[q(\tau + \tau_1)|k, \hat{m} = m]$ (remembering that the first pulse is of type k) can now be evaluated as the k th entry of the vector

$$\int_0^{T_M} Q^{\hat{m}}(\tau + \tau_1 - \tau_2)\mathbf{u}(\tau_2) d\tau_2.$$

In this equation $Q^{\hat{m}}$ denotes the m -fold convolution of $Q(\sigma)$ with itself.

At this point we note that the conditioning on \hat{m} enters in calculations of $A_q^k(\tau)$ for all k in the same manner, what can be used for a direct evaluation of $R_q(\tau)$. Let us define $R_q(\tau|\hat{m} = m)$ to denote $R_q(\tau)$ conditioned on the knowledge of \hat{m} . Now recalling (17), we get (in a convenient matrix notation)

$$R_q(\tau|\hat{m} = m) = \int_0^{T_M} \int_0^{T_M} \frac{\mathbf{u}^T(\tau_1)}{\hat{T}} \Theta \cdot Q^{\hat{m}}(\tau + \tau_1 - \tau_2)\mathbf{u}(\tau_2) d\tau_1 d\tau_2 \quad (20)$$

where $\Theta = \text{diag}(\Pi_k)$.

Step 2: Let $S_q^+(f)$ be the Fourier transform of $R_q(\tau|\hat{m} \geq 1)$ for $\tau > 0$, and $S_q^-(f)$ be the Fourier transform of the same autocorrelation for $\tau < 0$. For any $q(t)$ we have $S_q^-(f) = S_q^+(-f) = (S_q^+(f))^*$; we define $S_q^0(f)$ to be the Fourier transform of $R_q(\tau|\hat{m} = 0)$. Given that our conditioning on \hat{m} forms an event space

$$S_q(f) = S_q^+(f) + S_q^-(f) + S_q^0(f).$$

Next we write

$$S_q^+(f) = \lim_{M \rightarrow \infty} \int_0^{M\hat{T}} \sum_{\hat{m}=1}^M \int_0^{T_M} \int_0^{T_M} \frac{\mathbf{u}^T(\tau_1)}{\hat{T}} \Theta \cdot Q^{\hat{m}}(\tau + \tau_1 - \tau_2)\mathbf{u}(\tau_2) d\tau_1 d\tau_2 e^{-j2\pi f\tau} d\tau. \quad (21)$$

We define $\sigma = \tau + \tau_1 - \tau_2$ and recognize that for $\tau \in [0, M\hat{T}]$, $\sigma \in [-T_M, M\hat{T} + T_M]$. Observe that the limit of the integral over σ is not influenced by this change, since the integrand $Q^{\hat{m}}(\sigma) = 0$, for $\sigma \leq 0$; similarly, the limit of that integral is not changed by the addition of finite T_M to the upper limit of integration. Thus, we can set the order of integration as $\tau_1 \sigma \tau_2$; we can also multiply and divide the previous equation by $e^{-j2\pi f\tau_1} e^{j2\pi f\tau_2}$ in order to extract the Fourier transform $U(f)$ of $\mathbf{u}(\cdot)$ (and its conjugate transpose); the integrals over τ_1 and τ_2 are unaffected if the upper limit of integration is set to ∞ , since integrands are identically zero. Thus (21) becomes

$$S_q^+(f) = \frac{1}{\hat{T}} U^T(-f) \Theta \cdot \lim_{M \rightarrow \infty} \sum_{\hat{m}=1}^M \int_0^{M\hat{T}} Q^{\hat{m}}(\sigma) e^{-j2\pi f\sigma} d\sigma \cdot U(f), \quad (22)$$

Since the integral converges to the Fourier transform of $Q^{\hat{m}}$ (since the integrand is zero for $\sigma > MT_M$) we write

$$S_q^+(f) = \frac{1}{\hat{T}} U^T(-f) \Theta \left[\lim_{M \rightarrow \infty} \sum_{\hat{m}=1}^M (\hat{Q}(f))^{\hat{m}} \right] U(f) \quad (23)$$

where $\hat{Q}(f)$ is the Fourier transform of the matrix $Q(\sigma)$.

Step 3: From the construction, $\hat{Q}(f) = \text{diag}(e^{-j2\pi f T_k})P = \hat{\Delta}(f)P$. Recall that P has the eigenvalue $\lambda_1 = 1$, with the corresponding right eigenvector $v_1 = \mathbf{1}_n = [1, \dots, 1]^T$ and with the left eigenvector $w_1 = \mathbf{1}^T$; other eigenvalues $\lambda_k, k = 2, \dots, n$ have moduli strictly less than 1, and corresponding right eigenvectors v_k and left eigenvectors w_k . Let $\hat{\Lambda}_1(f)$ denote the eigenvalue of $\hat{Q}(f)$ with the largest magnitude. In the case of a synchronous chain, $\hat{\Lambda}_1(f) = e^{-j2\pi f T}$, and clearly $|\hat{\Lambda}_1(f)| = 1$ for all frequencies. If the chain is asynchronous, then $|\hat{\Lambda}_1(f)| = 1$ for frequencies that satisfy the following condition: for each ordered pair of $(T_k, T_l), T_k < T_l$ and $T_k = \ell_k \hat{T}, T_l = \ell_l \hat{T}$ (where \hat{T} is the greatest common divisor of all T_k), there exists an integer ι such that

$$\iota + f\ell_k \hat{T} = f\ell_l \hat{T}.$$

Clearly, for $f = k/\hat{T}, k \in \mathbb{N}$ the above equation is satisfied for $\iota = 0$ in all pairings of T_k, T_l , and $\hat{\Delta}(f) = I, \hat{\Lambda}_1 = \lambda_1 = 1$; we denote such frequencies as class A. The frequencies that satisfy the above condition for nonzero ι are said to belong to class B.

Step 4: The case when $|\hat{\Lambda}_1(f)| < 1$ is straightforward, as the geometric series involving $\hat{Q}(f)^{\hat{M}}$ converges, so we introduce

$$F(f) = \sum_{m=1}^{\infty} (\hat{Q}(f))^m \quad (24)$$

that equals

$$F(f) = (I - \hat{Q}(f))^{-1} - I = G(f) - I. \quad (25)$$

To complete evaluation of the continuous power spectrum, note that in the case of no transition during τ a procedure completely analogous to the one performed in the case of $\hat{m} > 0$ transitions yields

$$S_q^0 = \frac{1}{\hat{T}} U^T(-f) \Theta U(f). \quad (26)$$

Finally, by recalling $S_q(f) = S_q^+(f) + S_q^-(f) + S_q^0(f)$, we arrive at the spectral formula

$$S_{cq}(f) = \frac{1}{\hat{T}} U(f)^H [\Theta F(f) + (\Theta F(f))^H + \Theta] U(f). \quad (27)$$

The subscript c is used to emphasize that this is a continuous spectrum, i.e., the signal power is spread over all frequencies. By substituting $F = G - I$ in the above equation we recover (10).

Step 5: The case when $|\hat{\Lambda}_1|(f) = 1$ is considered next; note that this can happen only at frequencies when all entries in the diagonal matrix $\hat{\Delta}(f)$ (namely $e^{-j2\pi f T_\ell}$) are the same. We first decompose the matrix $\hat{Q}(f)$ using its eigenvectors

$$\hat{Q}(f) = e^{-j2\pi f T_\ell} \mathbf{1}_n \Pi + \sum_{k=2}^n \lambda_k e^{-j2\pi f T_\ell} v_k w_k^T.$$

Then

$$\sum_{\hat{m}=1}^M (\hat{Q}(f))^{\hat{m}} = \sum_{\hat{m}=1}^M (e^{-j2\pi f T_\ell})^{\hat{m}} \mathbf{1}_n \Pi + \Phi(f) \quad (28)$$

where

$$\Phi(f) = \sum_{k=2}^n \left(\frac{1 - (\lambda_k e^{-j2\pi f T_\ell})^{M+1}}{1 - \lambda_k e^{-j2\pi f T_\ell}} - 1 \right) v_k w_k^T. \quad (29)$$

Then, given $S_q(f) = S_q^+(f) + S_q^-(f) + S_q^0(f)$, we get

$$S_q(f) = \frac{1}{\tilde{T}} U^H(f) \Theta \cdot \lim_{M \rightarrow \infty} \left[\sum_{\hat{m}=-M}^M (e^{-j2\pi f T_\ell})^{\hat{m}} \mathbf{1}_n \Pi + \Phi(f) + \Phi^*(f) \right] \cdot U(f). \quad (30)$$

In this case

$$\lim_{M \rightarrow \infty} \Phi(f) = F(f) = \sum_{k=2}^n \frac{\lambda_k e^{-j2\pi f T_\ell}}{1 - \lambda_k e^{-j2\pi f T_\ell}} v_k w_k^T \quad (31)$$

and it will correspond to the continuous spectrum at f , as in (27).

In the case of a synchronous chain all T_k are equal to $T = \tilde{T}$, and the Poisson's equality establishes that

$$\lim_{M \rightarrow \infty} \sum_{\hat{m}=-M}^M (e^{-j2\pi f T})^{\hat{m}} = \frac{1}{T} \sum_{k=-\infty}^{\infty} \delta\left(f - \frac{k}{T}\right), \quad k \in \mathbb{N}. \quad (32)$$

In the case of an asynchronous chain the frequencies of interest are those yielding all $e^{-j2\pi f T_\ell}$ the same, defined previously as classes A and B. The frequencies in class B will have no contribution to the discrete spectrum for reasons clear from the Poisson equality ($\lim_{M \rightarrow \infty} \sum_{\hat{m}=-M}^M (e^{-j2\pi f T_\ell})^{\hat{m}} = 0$ $f \in$ class B). For all frequencies in class A ($f = k/\tilde{T}$, $k \in \mathbb{N}$) the limit will be the same for all k (as all summands are the same), so we can write

$$\lim_{M \rightarrow \infty} \sum_{\hat{m}=-M}^M (e^{-j2\pi f T_\ell})^{\hat{m}} = \frac{1}{T_0} \sum_{k=-\infty}^{\infty} \delta\left(f - \frac{k}{\tilde{T}}\right), \quad k \in \mathbb{N}. \quad (33)$$

where the constant T_0 will be determined next. Consider the $f = 0$ case—the impulse strength (or the “dc component”) will be [cf. (22)]

$$\lim_{M \rightarrow \infty} \frac{2M+1}{2M\tilde{T}} = \frac{1}{\tilde{T}}$$

so $T_0 = \tilde{T}$. The final result for the intensities of the impulses (“lines” in the discrete spectrum) equals (11), in agreement with [37]

$$S_{qd}\left(\frac{k}{\tilde{T}}\right) = \frac{1}{\tilde{T}^2} \left| \text{III}\left(\frac{k}{\tilde{T}}\right) \right|^2 \quad k \in \mathbb{N}, \quad (34)$$

ACKNOWLEDGMENT

The authors wish to acknowledge suggestions and clarifications offered by the reviewers, and in particular by Associate Editor J. Chiasson.

REFERENCES

- [1] G. Bilardi, R. Padovani, and G. L. Pierobon, “Spectral analysis of functions of Markov chains with applications,” *IEEE Trans. Commun.*, vol. COM-31, pp. 853–861, July 1983.
- [2] J. T. Boys, “Theoretical spectra of narrow-band random PWM waveform,” *IEE Proc.—Part B*, vol. 140, no. 6, pp. 383–400, 1993.
- [3] J. T. Boys and P. G. Handley, “Harmonic analysis of space vector modulated PWM waveforms,” *IEE Proc.—Part B*, vol. 137, no. 4, pp. 197–204, July 1990.
- [4] ———, “Spread spectrum switching—low noise modulation technique for PWM inverter drives,” *IEE Proc.—Part B*, vol. 139, no. 3, pp. 252–260, May 1992.
- [5] D. C. Champeney, *A Handbook of Fourier Transforms*. Cambridge, U.K.: Cambridge Univ. Press, 1987.
- [6] P. Galko and S. Pasupathy, “The mean power spectral density of Markov chain driven signals,” *IEEE Trans. Inform. Theory*, vol. IT-27, pp. 746–754, Nov. 1981.
- [7] T. G. Habetler and D. M. Divan, “Acoustic noise reduction in sinusoidal PWM drives using a randomly modulated carrier,” *IEEE Trans. Power Electron.*, vol. 6, pp. 356–363, July 1991.
- [8] P. G. Handley, M. Johnson, and J. T. Boys, “Elimination of tonal acoustic noise in chopper-controlled dc drives,” *Appl. Acoust.*, vol. 32, pp. 107–119, 1991.
- [9] D. L. Isaacson and R. W. Madsen, *Markov Chains: Theory and Applications*. New York: Wiley, 1976.
- [10] G. M. Jenkins and D. G. Watts, *Spectral Analysis and Its Applications*. Oakland, CA: Holden-Day, 1968.
- [11] J. G. Kassakian, M. F. Schlecht, and G. C. Verghese, *Principles of Power Electronics*. Reading, MA: Addison-Wesley, 1991.
- [12] J. G. Kemeny and J. L. Snell, *Finite Markov Chains*. Princeton, NJ: Van Nostrand, 1960.
- [13] R. L. Kirlin, S. Kwok, S. Legowski, and A. M. Trzynadlowski, “Power spectra of a PWM inverter with randomized pulse position,” *IEEE Trans. Power Electron.*, vol. 9, pp. 463–472, 1994.
- [14] L. Kleinrock, *Queueing Systems*. New York: Wiley, 1975.
- [15] S. Legowski, J. Bei, and A. M. Trzynadlowski, “Analysis and implementation of a grey-noise technique based on voltage space vectors,” in *IEEE APEC Proc.*, Feb. 1992, pp. 586–593.
- [16] S. Legowski and A. M. Trzynadlowski, “Hypersonic MOSFET-based power inverter with random pulse width modulation,” in *Proc. IEEE Ind. Applicat. Soc. Annu. Mtg.*, Oct. 1989, pp. 901–903.
- [17] ———, “Advanced random pulse width modulation technique for voltage-controlled inverter drive systems,” in *IEEE APEC Proc.*, Mar. 1991, p. 100–106.
- [18] A. Leon-Garcia, *Random Processes for Electrical Engineering*, 2nd ed. Reading, MA: Addison-Wesley, 1994.
- [19] H. Lev-Ari, “Nonstationary lattice-filter modeling,” Ph.D. dissertation, Electrical Eng. Dep., Stanford Univ., CA, 1983.
- [20] L. Ljung, *System Identification: Theory for the User*. Englewood Cliffs, NJ: Prentice-Hall, 1987.
- [21] S. L. Marple, *Digital Spectral Analysis with Applications*. Englewood Cliffs, NJ: Prentice-Hall, 1987.
- [22] D. Middleton, *An Introduction to Statistical Communication Theory*. New York: McGraw-Hill, 1960.
- [23] A. V. Oppenheim and R. W. Schaffer, *Discrete-Time Signal Processing*. Englewood Cliffs, NJ: Prentice-Hall, 1989.
- [24] A. Papoulis, *Probability, Random Variables and Stochastic Processes*, 2nd ed. New York: McGraw-Hill, 1984.
- [25] J. K. Pedersen and F. Blaabjerg, “Implementation and test of a digital quasi-random modulated SFAVM PWM in a high-performance drive system,” in *Proc. IEEE Ind. Electron. Conf. IECON*, 1992.

- [26] J. G. Proakis and D. G. Manolakis, *Digital Signal Processing: Principles, Algorithms and Applications*. New York: Macmillan, 1992.
- [27] J. M. Retif and B. Allard., "A PWW ASIC using stochastic coding," in *PESC Proc.*, July 1992, pp. 587–594.
- [28] A. M. Stanković, "Random pulse modulation with applications to power electronic converters," Ph.D. dissertation, Electrical Eng., Comput. Sci. Dep., Massachusetts Inst. Technol., Cambridge, 1993.
- [29] A. M. Stanković, G. C. Verghese, and D. J. Perreault, "Analysis and synthesis of random modulation schemes for power converters," in *PESC Proc.*, June 1993, pp. 1068–1074.
- [30] ———, "Analysis and synthesis of random modulation schemes for power converters," *IEEE Trans. Power Electron.*, vol. 10, pp. 680–693, Nov. 1995.
- [31] T. Tanaka and T. Ninomiya, "Random-switching control for dc-dc converter: Analysis of noise spectrum," in *IEEE PESC Proc.*, 1992, pp. 579–586.
- [32] T. Tanaka, T. Ninomiya, and K. Harada, "Random-switching control in dc-dc converters," in *IEEE PESC Proc.*, 1989, pp. 500–507.
- [33] A. M. Trzynadlowski, F. Blaabjerg, J. K. Pedersen, R. L. Kirlin, and S. Legowski, "Random pulse width modulation techniques for converter-fed drive systems—A review," *IEEE Trans. Ind. Applicat.*, vol. 30, pp. 1166–1175, 1994.
- [34] A. M. Trzynadlowski, S. Ji, and S. Legowski, "Random pulse width modulation of delta inverter for automotive applications," in *Proc. IEEE Ind. Applicat. Soc. Annu. Mtg.*, Oct 1991, pp. 826–833.
- [35] A. M. Trzynadlowski, S. Legowski, and R. L. Kirlin, "Random pulse width modulation technique for voltage-controlled power inverters," in *Proc. IEEE Ind. Applicat. Soc. Annu. Mtg.*, Oct 1987, pp. 863–868.
- [36] A. M. Yaglom, *Correlation Theory of Stationary and Related Random Functions*. New York: Springer-Verlag, 1987.
- [37] Y. Yoshida, "Method of power spectrum calculation of Markov signals," *Electron. Commun. Japan*, vol. 56-A, no. 9, pp. 64–73, 1973.



Aleksandar M. Stanković (S'88–M'91) received the Dipl. Ing. degree from the University of Belgrade, Yugoslavia, in 1982, the M.S. degree from the same institution in 1986, and the Ph.D. degree from Massachusetts Institute of Technology, Cambridge, in 1993, all in electrical engineering.

He has been an Assistant Professor with the Department of Electrical and Computer Engineering at Northeastern University, Boston, since 1993. His research interests include modeling and control problems in power electronics and power systems.

Dr. Stanković is a member of the IEEE Power Electronics, Control Systems, and Power Engineering Societies.



George C. Verghese (S'74–M'78) received the B. Tech. degree from the Indian Institute of Technology at Madras in 1974, the M.S. degree from the State University of New York at Stony Brook in 1975, and the Ph.D. degree from Stanford University, CA, in 1979, all in electrical engineering.

He is Professor of Electrical Engineering and a Member of the Laboratory for Electromagnetic and Electronic Systems at the Massachusetts Institute of Technology, Cambridge, which he joined in 1979.

He is coauthor of *Principles of Power Electronics* (Reading, MA: Addison-Wesley, 1991). His research interests include systems, control, and estimation, especially as applied to power electronics, electrical machines, and large power systems.

Dr. Verghese has served as an Associate Editor of *Automatica*, the IEEE TRANSACTIONS ON AUTOMATIC CONTROL, and (currently) the IEEE TRANSACTIONS ON CONTROL SYSTEMS TECHNOLOGY. He has served on the AdCom and other committees of the IEEE Power Electronics Society, and also as Founding Chair of its technical committee and workshop on Computers in Power Electronics.



David J. Perreault received the B.S. degree from Boston University, MA, in 1989, and the M.S. degree from Massachusetts Institute of Technology (MIT), Cambridge, in 1991, both in electrical engineering. He is currently a Ph.D. candidate at MIT.

He is a Research Assistant in the MIT Laboratory for Electromagnetic and Electronic Systems, where he is engaged in research and development of cellular power electronic architectures.

Mr. Perreault is a member of Tau Beta Pi and the National Society of Professional Engineers, and was the recipient of the IEEE Convergence Fellowship in Transportation Electronics.